3. Methods

3.1. Seismic methods

The study relies on 171 reflection seismic profiles (**Fig. 1**) and a 3D seismic volume, the location of which is kept confidential, provided by CGX Energy Inc. Both were tied to 39 wells.

A detailed interpretation of several seismic sections was made to connect the distal continental margin penetrated by industrial wells with adjacent oceanic crust of the Offshore Guyana Block, using any stratigraphic division provided by the respective well report. Furthermore, the interpretation of the entire seismic grid was made, resulting in the following seismostratigraphic units, which we could map in the entire study area (**Fig. 4**):

1) unit between the sea-bottom and the Lower Miocene base of the main prograding wedge

2) unit between the wedge base and top of the Lower Eocene carbonates

3) unit between the top of the Lower Eocene carbonates and the “Santonian” unconformity

4) unit between the “Santonian” unconformity and the late Aptian-Albian Equatorial Atlantic break-up unconformity

5) unit between the break-up unconformity and the intra lower Lower Cretaceous marker (Potoco Formation)

6) unit between Lower Cretaceous marker (Potoco Formation) and the top Jurassic marker

7) unit between the top Jurassic marker and basement.

The units were tied to wells and mapped in seismic images as based on their characteristic image and character of their boundaries.

Unit 1 is the only unit with the internal reflector pattern, which indicates a massive progradation on the slope. It is deformed by the gravity glide system detached inside the Upper Cretaceous sediments. It is the only unit that experienced a large oceanward shift of the shelf break, in the order of 13-60 km. Its basal portion on the shelf is characterized by a pale structureless zone lacking distinct parallel reflectors. The base of this unit onlaps on the underlying distinct erosional unconformity developed on the shelf.

Unit 2 can be characterized as highly reflective in its shelf portion where its reflectors are parallel. It has a distinct aggradation pattern in the shelf break region. Its upper boundary in the shelf region is formed by erosional unconformity. Its basal portion occasionally onlaps onto the underlying strata. This unit seals the youngest faults developed by the regional stresses.

Unit 3 probably has the least parallel character of reflectors in the shelf region. Its reflectors are not particularly strong either. This unit contains a large amount of channels at different levels. Its basal portion overlies a pronounced unconformity in shelf and upper slope regions.

Unit 4 has its upper portion with a seismic character rather similar to that of Unit 3. Its lower portion, however, is rather reflective, formed by a set of parallel reflectors. It onlaps the underlying Equatorial Atlantic unconformity developed on shelf and upper slope.

Unit 5 is rather reflective and characterized by parallel reflectors on the shelf. It contains numerous faults that die out towards its top. Some of them are associated with localized reflector packages thickening towards them. The basal portion of this unit is imaged as reflectors onlapping a rather strong and regionally extensive reflection.

Unit 6 onlaps the basement. The basement is characterized by a rather isotropic image and erosional unconformity at its top. Unit 6 is represented by parallel sets of relatively distinct reflectors, locally diverging towards faults.

Apart from these units, we made a short-distance horizon determination in seismic sections, which were tied to local wells, using the formation names and ages determined in respective well. They will be shown in individual profiles later.

3.2. Gravity methods

The input for our gravity database came from the following sources:

1) NGDC (National Geophysical Data Center) ship track data (http://www.ngdc.noaa.gov/mgg/geodas/trackline.html). Their resolution was highly variable.
2) EGM08 (Earth Gravity Model 2008), a joint effort of geodesists to produce a 2 arc-minute (~3.7 km) resolution world gravity model of harmonic degree 2190 (http://earth-info.nga.mil/GandG/wgs84/gravitymod/egm2008/index.html). The actual data resolution was about 9.1 kilometers. These data were used onshore.
3) Satellite-derived marine gravity (Version DNSC08) (http://www.space.dtu.dk/English/Research/Scientific_data_and_models/Global_Marine_Gravity_Field.aspx). This source contained a 1 arc-minute (~2 km) resolution data grid over the world.
4) Point gravity data over the United States with variable spatial resolution (http://gis.utep.edu/index.php?option=com_content&view=article&id=197%3Agdrp-home&catid=51%3Amain-site&Itemid=54).

The data were integrated at the grid level for the entire study area. The Bouguer correction was made with a density of 2670 kgm^{-3} onshore and 2200 kgm^{-3} offshore. The Isostatic Anomaly was produced using an isostatic correction grid produced using the Airy hypothesis. The density contrast used for the Moho discontinuity was 340 kgm^{-3}. All data were leveled relative to EGM08 in the WGS84 geographic datum.

The Free-air data, corrected only for the latitude and elevation of the measurement location relative to mean sea level, were reliable in flat-topography regions. They managed to highlight the flow lines representing the spreading direction of the oceanic crust in the deep

oceanic basin. These images also highlighted the boundary between continental and oceanic crusts by containing a maximum for the continent near the crustal boundary and minimum for the ocean near the boundary, although the boundary was not exactly located, being affected by a number of factors apart from just deep crustal contrasts (see Watts & Stewart 1998).

The Bouguer data represent more enhanced gravity imaging. Apart from oceanic flow lines and continental crust/oceanic crust boundary, they allowed one to interpret the crustal architecture, although they had inherited problems such as large compensated topographic highs onshore sometimes appearing as gravity lows, similar to basins.

The Isostatic residual gravity anomaly data represent the most enhanced gravity imaging. They were supposed to handle the onshore Bouguer anomaly problem by assuming that the excess mass of large topographic highs is Airy-compensated by a reduction in mass below the high. This data set allowed us to interpret the boundaries of crustal blocks and their architecture, especially when it was further enhanced by various wavelength filters and mathematical treatment.

The treatment resulted in the two types of spatial derivatives. The first vertical derivative display was meant to enhance fault features and dipping boundaries, indicated by changes from negative to positive anomalies, or vice versa. The down-thrown side should be indicated by negative values. The total horizontal derivatives were calculated from a combination of simultaneous derivatives in orthogonal directions. Maxima in the total horizontal derivative display of the Isostatic residual gravity anomaly data should indicate fault locations more exactly than the first vertical derivative display, although the displays are complimentary to each other.

3.3. Magnetic methods

The input for our magnetic database came from the following sources:

1) Magnetic Crustal Field model from NOAA/NGDC (http://www.ngdc.noaa.gov/seg/EMM/emm.shtml). It is a 15 arc-minute (28 km) resolution grid produced from a 720 degree harmonic model of the earth's magnetic field.
   The model is derived from a satellite magnetic field model integrated with higher resolution data.
2) World Digital Magnetic Anomaly Map (http://projects.gtk.fi/WDMAM/). It is a 3 arc-minute (0.05 degree, 5.5 km) resolution data grid with regional data grids and a grid of the NGDC track line data.
3) EMAG2 from the NGDC with a resolution of 2 arc-minutes (http://geomag.org/models/emag2.html).
4) The North America Magnetic Grid from with a resolution of 1 kilometer (http://tin.er.usgs.gov/magnetic/).

The data were integrated at the grid level for the entire study area. Data from sources 1 and 2 were used to fill the gaps in the EMAG2 database. All data were leveled relative to EMAG2 in the WGS84 geographic datum. Our final result was the Total magnetic field map, delivered in the ArcGIS format at a 15 arc-second (~500 meter) resolution.

Total magnetic field data were another useful data set for the crustal boundary determination. This was because the magnetic susceptibility of different crustal rocks is controlled by the susceptibility of their composing minerals. For example, (Lillie, 1999) illustrates that peridotites, basalts and gabbros, which are the most typical rocks of the oceanic and proto-oceanic crusts, have magnetic susceptibilities, which are at least one magnitude larger than the susceptibilities of diorite, and granite, which are typical for continental crust.

Because the total magnetic field anomaly is calculated by subtracting the magnitude of the ambient magnetic field from the magnitude of the total magnetic field, the same magnetic body would have a different anomaly at different locations in the globe (Lillie 1999). Because our study area is in the equatorial region, the induced field opposes the ambient field at the surface directly over the body, leading to a magnetic anomaly overlapping the location of its source, which makes the interpretation relatively straightforward.

Apart from attempts to find anomalies imaging the boundary of continental and oceanic crusts, we were interpreting also prominent magnetic anomalies along oceanic fracture zones, following the examples from Cochran (1973), Fainstein *et al*. (1975) and Cande & Rabinowicz (1979). These anomalies were explained by large quantities of serpentinized peridotites from the upper mantle along them (Thompson & Melson 1972; Bonatti 1976, 1978). In accordance with Karner (2000), we used the landward ends of anomalies associated with oceanic fracture zones for the determination of the oceanic/continental crust boundary. This criterion, however, was not as exact as criteria provided by gravity methods, because of the potential presence of mafic intrusions in the distal continental margin.

6. Discussion

The discussion of the southern terminus of the Central Atlantic oceanic segment would benefit from the discussion of the interaction among the Central, South and Equatorial Atlantic oceans and the control by the pre-existing anisotropy on this interaction. For example, there are numerous published evidences about the pre-existing fault zones making the rifting in the northernmost portion of the South Atlantic rift system complex (e.g. Jardim de Sá 1984; de Matos 1987; Chang *et al*. 1988). These fault zones were part of the Braziliano-Pan-African terrains reworked by Proterozoic orogeny. They are represented by the Borborema province in Brazil and the Nigerian Shield/Nigerian Pan-African belt in Africa.

The initial rifting in this region started during the Late Jurassic (Chang *et al*. 1988). It was either coeval or slightly younger than the continental break-up in the Offshore Guyana Block. The northward propagation of the South Atlantic rift systems did not make it through the Patos fault zone during this time. This is indicated by the presence of the Upper Jurassic

sediments in the Jatobá-Tucano-Recôncavo, Sergipe-Alagoas and Araripe basins to the south and their lack in the Rio de Peixe and Potiguar basins to the north of the Patos fault zone. The Pernambuco-Ngaoundere fault zone, which was located 150 km south of the Patos fault zone, also acted as part of the same rift-propagation terminus.

A large width of the shallow Late Jurassic basin to the south of the Patos and Pernambuco-Ngaoundere fault zones indicates an extension affecting a large area. To the north of these zones, the extension resulted only in a dyke development in the Borborema province and the Paleozoic Parnaiba Basin (Almeida *et al*. 1988; de Matos 1992). This dramatic N-S change indicates that the Patos and Pernambuco-Ngaoundere fault zones were active as accommodation zones and weak enough to stop the propagation of the South Atlantic rift system into the region north of them.

The main rift phase took place during the Neocomian – early Barremian (Chang *et al*. 1988). This phase did not succeed in propagating the rift system beyond the Pernambuco-Ngaoundere fault zone either. However, the extensional deformation jumped into a northwestern region. It formed a number of intra-cratonic basins along the Cariri-onshore Potiguar trend to bypass the problem with propagating through the pre-existing Pernambuco-Ngaoundere and Patos fault zones, which kept using the accumulated stresses for their reactivation, preventing the South Atlantic rift system from further propagation. This also documents that the main E-W trending strike-slip fault zones, such as the Pernambuco-Ngaoundere and Patos, continued behaving as a large complex accommodation zone, balancing extensional deformation in the Jatobá-Tucano-Recôncavo and Sergipe-Alagoas rift zones with coeval extension in the intra-cratonic rift branch of the Cariri-Potiguar trend. This trend is exactly parallel to the Pan-African fold belt and its thrust faults, which are occurring in the Borborema province.

The Neocomian – early Barremian rifting was followed by the late Barremian rifting. It was characterized by extension culmination in the northern rift zones of the South Atlantic rift system (Chang *et al*. 1988). It represented the final rifting stages in the Jatobá-Tucano-Recôncavo and Sergipe-Alagoas rift zones, and intra-cratonic rift basins located to the south of the Pernambuco-Ngaoundere strike-slip system. It also represented a major change in the controlling dynamics and the rift initiation in eastern Equatorial Atlantic domain, associated with a change from the NW-SE striking regional extension to WNW-ESE extension during this phase. During this time, the rifting in the Cariri Valley and onshore Potiguar basins was aborted.

The rifting initiation in the eastern Equatorial Atlantic domain was coeval with continuous deposition in the offshore Potiguar Basin. Evidences for this initiation come from the Benue Trough in Nigeria (Benkhelil et al. 1988; Popoff 1988). During this time, the WNW-ESE extension, which was characteristic for the NE Brazilian corner, reactivated the pre-existing NE-SW striking normal faults of the Potiguar Basin as sinistral transtensional strike-slip faults. New grabens opened during the late Barremian on the Aracati Platform to the west of the Potiguar Basin. They were controlled by normal faults perpendicular to the new direction of extension.

The late Barremian rifting was followed by the Aptian rifting that reached the region of all future Equatorial Atlantic basins (Souza 1982; de Matos 1992). The most interesting Aptian situation was present in the Pernambuco-Paraiba Basin region. This region was affected by a large number of roughly E-W striking dextral strike-slip faults. They formed a 340 km wide deformation zone to the south of the E-W trending future break-up trajectory in the offshore Potiguar Basin. At least some of them were the reactivated pre-existing transfer faults of the Braziliano orogen. This region was also deformed by numerous coeval NE-SW striking sinistral strike-slip faults. They were formed along the pre-existing thrusts of the Braziliano orogen. Both sets of faults acted as a conjugate set. They were linked by smaller normal faults and oblique-slip faults.

It was during the Aptian when the northern tip of the South Atlantic rift system "breached" the Pernambuco-Ngaoundere strike-slip fault zone and resumed its northward propagation. This is documented by syn-rift seismostratigraphy of small half-grabens in seismic cross sections cutting though the Pernambuco Plateau (Gomes *et al*. 2000; Nemčok *et al*. 2004) and proven Aptian sediments in a small NNE-SSW trending half-graben in the Cabo sub-basin of the Pernambuco-Paraiba Basin (de Matos 1987). The entire Touros Platform between the onshore Potiguar Basin and the Patos Fault Zone apparently behaved as the accommodation zone between the rifting in the northernmost South Atlantic system and the Equatorial Atlantic rift system for a little longer (de Matos *et al*. 1987).

We believe that the aforementioned delay in rift propagation in this region was caused by a dextral strike-slip linkage of the Potiguar Basin with the Benue Trough, which prevented the remaining continental bridge from undergoing rifting. It was the northward propagation of both the NE-SW trending Sergipe-Alagoas sinistral strike-slip and roughly N-S trending normal fault systems, which made it through this last continental bridge located between the offshore Potiguar-Benue trend and the Patos dextral strike-slip fault zone, along the future Pernambuco-Paraiba segment of the South Atlantic (Rosendahl *et al*. 2005).

The rift-drift transition in the Pernambuco-Paraiba Basin did not happen until the Aptian/Albian transition. However, the data on the continental break-up timing in this area are not direct. The timing is implied, using a marine transgression, which initiated at about the Aptian/Albian transition, according to available biostratigraphic data (Noguti & Santos 1972; Dias-Brito 1987), as a constraint. This rift-drift transition completed the rifting of the Southern Atlantic affected by pre-existing anisotropy.

In order to think about a rate of the South Atlantic opening, we can take its length of 3 560 km between the central offshore Namibia and central offshore Cameroon. Given the oldest crustal age constraints from Müller *et al*. (1993, 1997, 2008), we can derive that the opening lasted from 130-135 to 115-120 Ma, having a rate of 0.24 my^{-1}.

Repeating the same exercise for the Main body of the Central Atlantic, we can take its length of 3 480 km between the Guinea Plateau and the southernmost tip of Portugal and find out that its opening took place roughly from the Hettangian to Callovian, having a rate of 0.08 my^{-1}. The difference of 0.16 my^{-1} is not much, making the Central and South Atlantic oceans comparable with respect to the opening rate.

A comparison of the earlier discussion with Interpretation sub-chapter allows us to see how both oceans fought with their terminuses. The South Atlantic took the Late Jurassic-Aptian time to breach through a large system of roughly perpendicular dextral strike-slip fault zones and other related faults, almost going for a “breaching one at the time” mechanism. The Central Atlantic had similar problems with a large system of roughly perpendicular sinistral strike-slip fault zones and related faults in its southern terminus, and developed laterally offset Gulf of Mexico and proto-Caribbean oceanic corridors without managing to extensionally break its southern terminus.

In order to understand why the Offshore Guyana Block did not propagate further south along its trend after having a length of time similar to that of the northernmost South Atlantic for making it, we need to return to the point of discussion when the South Atlantic tried to make it through the reactivated Pernambuco-Ngaoundere and Patos strike-slip fault zones and made a Neocomian – early Barremian lateral jump to the NW, into the Cariri-Potiguar trend (see Chang *et al*. 1988), although in the South Atlantic case, the original trend eventually made it through. Although our data indicate rifting attempts along the Central Atlantic trend inside the Guyana Shield, it was rift zones to the NW of this trend, in the Gulf of Mexico and proto-Caribbean regions, which reached sea-floor spreading for limited time periods. While the former stopped oceanic crust accretion by 145-35 Ma, the latter would continue if it was not consumed by the subduction sometimes by end of Cretaceous (see Seton *et al*. 2012 and references therein).

Now we can turn to the point of our discussion where we left the South Atlantic being completely opened and its western continuation, the Equatorial Atlantic, starting to propagate. This was during the Aptian/Albian transition according to biostratigraphic constraints (Noguti & Santos 1972; Dias-Brito 1987), during the same time when the biostratigraphic constraints from wells indicate a development of the break-up unconformity on the Demerara Plateau.

In fact, the initial propagation of the intra-continental strike-slip zones in the Equatorial Atlantic region from the east to the west started earlier than that (e.g. Szatmari 2000). The onset is of the late Barremian age (e.g. Popoff 1988; de Matos 1992; Guiraud & Maurin 1992), based on the age of the basal transgressive sediments in the Benue Trough, and ages of the later syn-rift sediments on the Brazilian continent and in the Ivory Coast coastal area. The northernmost South Atlantic must have been waiting with breaching through the Touros Platform until the Aptian/Albian transition because of a very effective stress release along the dextral strike-slip linkage of the Potiguar Basin with the Benue Trough.

In the meantime, the westward propagation of the Equatorial Atlantic rifting took place. It can be demonstrated as based on younging basal sediments in basins on the Brazilian side of the system. The Potiguar Basin does not have a fine enough stratigraphic resolution to indicate the exact time within the Aptian stage but it indicates that the Aptian sediments rest on the Neocomian sediments transgressively (de Azevedo 1991). The oldest sediments of the Mundaú sub-basin of the Ceará Basin have an early Aptian age (Costa *et al*. 1990). Studies available from the Barreirinhas Basin, Gurupí graben system and Para Maranhão Basin do not have fine resolution and, therefore, they only document the Aptian age of basal sediments

(Cainelli *et al*. 1986; de Azevedo 1991). The westernmost basins, including the Marajo and Foz do Amazonas basins, have their basal sediments as old as the Aptian/Albian boundary and the upper Aptian-Albian, respectively (de Azevedo 1991). Based on these rough data, we can interpret that the westward propagation of rifting in the future Equatorial Atlantic, controlled by the overall dextral transtension, took place over approximately 10-11 Ma. When we take the oceanic crust age constraints from Müller *et al*. (1993, 1997, 2008), we find out that it took about 5 Ma for a 3 090 km long system to propagate, giving us a rate of 0.62 my^{-1}. This rate is 0.4 and 0.48 my^{-1} faster than the rates of the South and Central Atlantic oceans, respectively, making these two similar to each other and the Equatorial Atlantic one different from them, being much faster.

Our discussion so far portrays a picture of:

1) both the Central and Southern Atlantic oceans having problems with their southern and northern terminuses, respectively, from the Callovian-Oxfordian to the late Barremian;
2) the Southern Atlantic propagating a distance between the Pernambuco-Ngaoundere fault zone and the zone, which was linking the Potiguar Basin and the Benue Trough; and
3) the Central Atlantic oceanic segment failing to propagate along its trend.

Subsequently, from the late Barremian till the Aptian/Albian transition, both terminuses have been linked by the system of strike-slip fault zones and pull-apart basin terrains progressively used for the E-to-W Equatorial Atlantic propagation from the South Atlantic to the Central Atlantic. The comparison of propagation rates indicates that relatively slowly propagating South and Central Atlantic oceans became hard-linked by the Equatorial Atlantic relatively quickly. While the Equatorial Atlantic linked with the northernmost tip of the South Atlantic, it did not link with the southernmost tip of the Central Atlantic oceanic segment. On the contrary, it linked with the Central Atlantic at latitude of the future boundary between the Demerara and Guinea plateaus, separating the Offshore Guyana Block from the remaining portion of the Central Atlantic, termed here the Main body of the Central Atlantic.

Described linkage of the Central and South Atlantic oceans roughly resembles a linkage of the two tensile fractures in a brittle layer (see Pollard & Aydin 1988; **Fig. 10**) where the fractures reach a small overstep and eventually develop hard linkage that links a propagation tip of one fracture with a point inside of the other one. Despite of the scale difference, the propagation and linkage processes affect brittle layers in both cases, because the observable geometry of the oceanic system is exhibited by the deformed layer of the bounding upper continental crust. The difference is represented by the fact that the Equatorial Atlantic did not propagate through the lithosphere characterized by the homogeneous upper crustal layer but its upper crustal propagation was influenced by a system of pre-existing anisotropies.

When we look at details of the Equatorial Atlantic geometry, we can observe that the tectonic stresses created a right-stepping system of ENE-WSW dextral strike-slip fault zones and pull-apart basin systems between them. P shear orientation of dextral fault zones instead of R shear orientation (sensu Christie-Blick & Biddle 1985; Naylor *et al*. 1986) indicates that either they

were not initiated by transtensional stress or their positions were affected by prominent crustal weaknesses of NE-SW strikes associated with Proterozoic and Paleozoic orogenies (e.g. Mascle *et al*. 1988; Genik 1992; Guiraud & Maurin 1992). For example, the Late Cretaceous reactivation of the NE-SW striking Sobral-Pedro II Fault in the Borborema province to the south of the Barreirinhas Basin (Miranda *et al*. 1986) serves as a support for the latter argument. Furthermore, a similar dextral reactivation of the NNE-SSW striking Pan-African shear zones was reported from Nigeria (Ball 1980; Caby 1989).

When the rifting along the future Equatorial Atlantic between the late Barremian and Aptian/Albian transition linked the Central Atlantic with propagating South Atlantic, it must have further helped the southern terminus of the Central Atlantic Ocean to resist the Central Atlantic propagation along its trend. The help from the Equatorial Atlantic must have become decisive after it opened, separating the Offshore Guyana Block from the Main body of the Central Atlantic, rotating it in a dextral sense.

The initial separation of the Offshore Guyana Block from the Main body of the Central Atlantic was the time when the entire fault activity in the Offshore Guyana Block terminated. This also was the time when a large proportion of faults in the distal Guyana margin segment stopped their activity as well. A subsequent progressive dextral rotation of the South American Plate together with the Offshore Guyana Block must have brought the system of perpendicular strike-slip fault zones of this ocean terminus into less favorable geometries for reactivation by the existing regional stress field, which is indicated by their successive activity terminations between the Aptian/Albian transition and early Eocene, with progressively less and less of them remaining active till the end of this period. In the same time, the sea-floor spreading of the Equatorial Atlantic to the south of the Main body of the Central Atlantic prevented the Central Atlantic from any attempts to propagate further south along its trend.

In accordance with observations of multiple dextral strike-slip faults at strike-slip-controlled segments of the Equatorial Atlantic margins (e.g. Marinho *et al*. 1988; Basile *et al*. 1998; Benkhelil *et al*. 1998; Nemčok *et al*. 2012), the separation of the Offshore Guyana Block from the Main body of the Central Atlantic by the propagating Equatorial Atlantic must have been also attempted along a system of strike-slip faults, rather than a single one. This situation is most likely indicated by a deformation zone including several ridges and troughs, which we believe is located to the north of the eastern triangular end of the Accommodation Block. Suggested ridges and troughs are imaged by the Free-air gravity map (**Fig. 1a**) as a system of ENE-WSW to NE-SW trending positive and negative anomalies. We assume that it is a highly deformed character of the oceanic crust in this zone that disrupts a typical magnetic stripe anomaly image in this small area, and believe that this causes a small mistake in maps of Müller *et al*. (1993, 1997), assigning the Aptian-Santonian age (109-84 Ma) to this piece of oceanic crust (see **Fig. 2**). Our reconstruction (**Fig. 9**) indicates that the northern boundary of the Accommodation Block runs southeast to meet the very southwestern tip of the Guinea Plateau instead of meeting it at a bit northern location. Unlike in the case of the Offshore Guyana Block, we do not have direct well and seismic evidences supporting our version of the oceanic crust age in this small zone, but offer an alternative interpretation, which explains

the images provided by various gravity maps better and is in accordance with our detailed reconstruction of the Accommodation Block development.

Extra references (on top of those in article)

ALMEIDA, F. F. M., DAL RE CARNEIRO, C., MACHADO, D. D. L., JR. & DEHIRA, L. K. 1988. Magmatismo Pos-Paleozoico no nordeste oriental do Brasil. Post-Paleozoic magmatism of the eastern part of northeastern Brazil. *Revista Brasileira de Geociencias*, **18**, 451-462.

BONATTI, E. 1976. Serpentinite protrusions in the oceanic crust. *Earth and Planetary Science Letters*, **32**, 107-113.

BONATTI, E. 1978. Vertical tectonism in oceanic fracture zones. *Earth and Planetary Science Letters*, **37**, 369-379.

CANDE, S. C. & RABINOWICZ, P. D. 1979. Magnetic anomalies of the continental margin of Brazil. AAPG, Tulsa.

COCHRAN, J. R. 1973. Gravity and Magnetic Investigations in the Guiana Basin, Western Equatorial Atlantic. *Geological Society of America Bulletin*, **84**, 3249-3268.

DIAS-BRITO, D. 1987. A Bacia de Campos no Mesocretaceo; uma contribuicao a paleoceanografia do Atlantico sul primitivo. The Campos Basin of the Middle Cretaceous; a contribution to paleo-oceanography of the ancient South Atlantic. *In*: CARNEIRO, C.D.R. (ed.) *Revista Brasileira de Geociencias*, 162-167.

FAINSTEIN, R., MILLIMAN, J.D. & JOST, H. 1975. Magnetic character of the Brazilian continental shelf and upper slope. *Revista Brasileira de Geociencias*, **5**, 198-211.

KARNER, G. D. 2000. Rifts of the Campos and Santos Basins, Southeastern Brazil: Distribution and timing. *In*: MELLO, M. R. & KATZ, B. J. (eds) *Petroleum systems of South Atlantic margins*. AAPG Memoir, **73**, 301-315.

LILLIE, R. J. 1999. *Whole Earth Geophysics. An Introductory Textbook for Geologists and Geophysicists*. Prentice Hall, Upper Saddle River.

Noguti, I. & Santos, J. F. D. 1972. Zoneamento preliminar por foraminiferos planctonicos do aptiano ao mioceano na plataforma continental do Brasil. Preliminary zoning of planktonic foraminifera of the Aptian to Miocene rocks of the continental shelf of Brazil. *Boletim Tecnico da PETROBRAS*, **15**, 265-283.

SOUZA, J. M. 1982. *Transmission of seismic energy through the Brazilian Parana Basin layered basalt stack.* Master's Thesis, University of Texas at Austin, Austin.

SZATMARI, P. 2000. Habitat of petroleum along the South Atlantic margins. *In*: MELLO, M. R. & KATZ, B. J. (eds) *Petroleum Systems of South Atlantic Margins*. AAPG Memoir, **73**, 69–75.

THOMPSON, G. & MELSON, W. G. 1972. The petrology of oceanic crust across fracture zones in the Atlantic Ocean; evidence of a new kind of sea-floor spreading. *Journal of Geology*, **80**, 526-538.

WATTS, A. B. & STEWART, J. 1998. Gravity anomalies and segmentation of the continental margin offshore West Africa. *Earth and Planetary Science Letters*, **156**, 239-252.

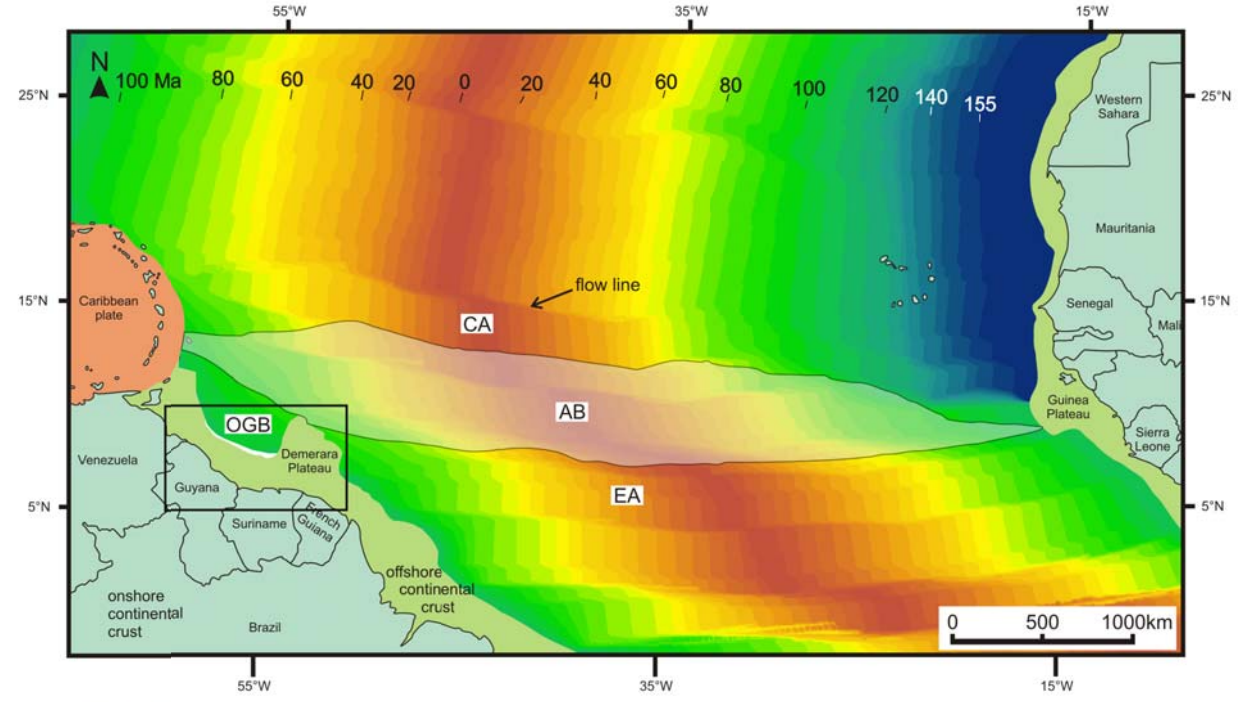
55°W
35°W
15°W
25°N
15°N
5°N
N
100 Ma
80
60
40
20
0
20
40
60
80
100
120
140
155
Western Sahara
Mauritania
Senegal
Mali
Guinea Plateau
Sierra Leone
Caribbean plate
flow line
CA
AB
EA
OGB
Demerara Plateau
Venezuela
Guyana
Suriname
French Guiana
Brazil
onshore continental crust
offshore continental crust
0
500
1000km
1
2

Guyana- Suriname Basin

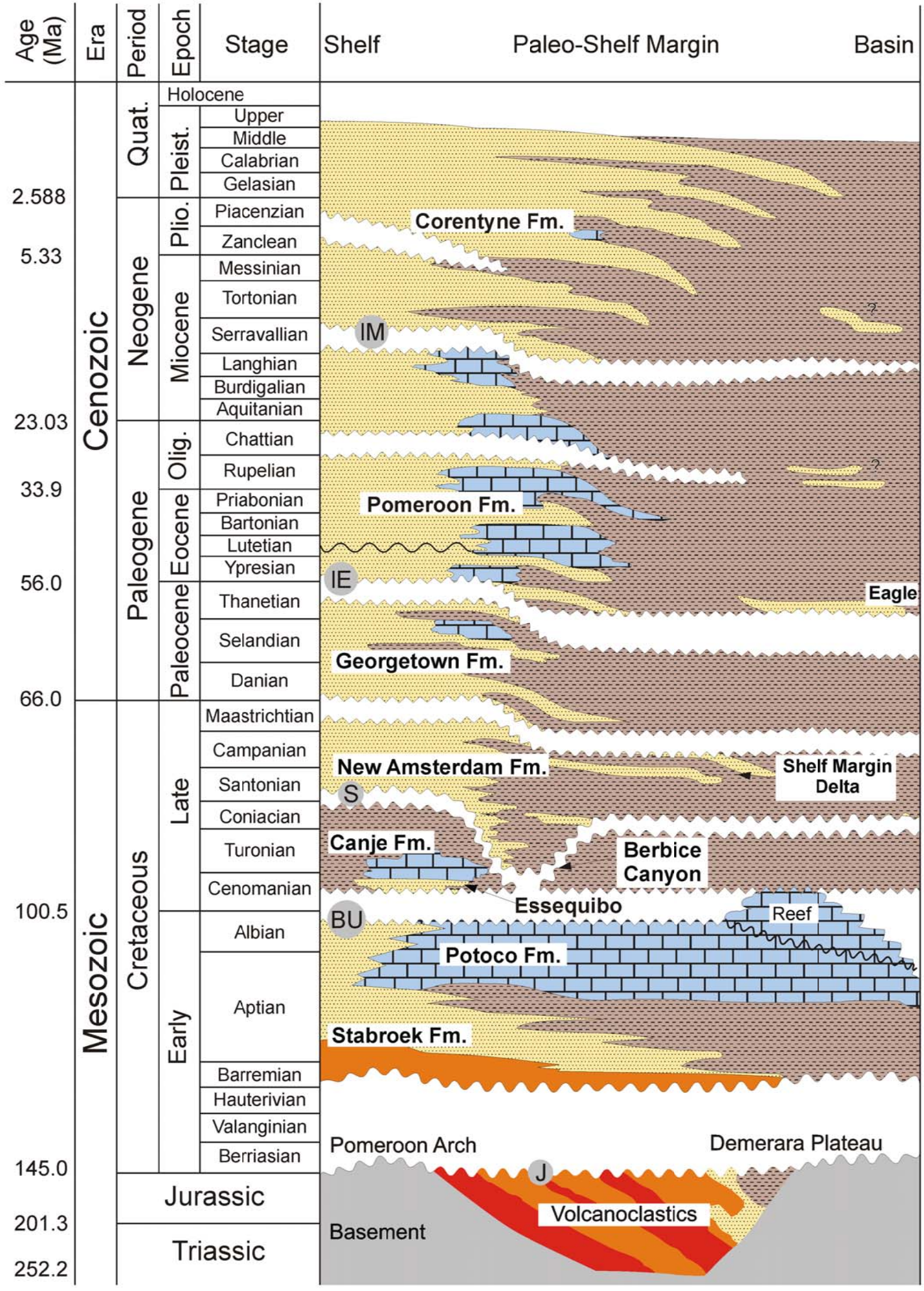

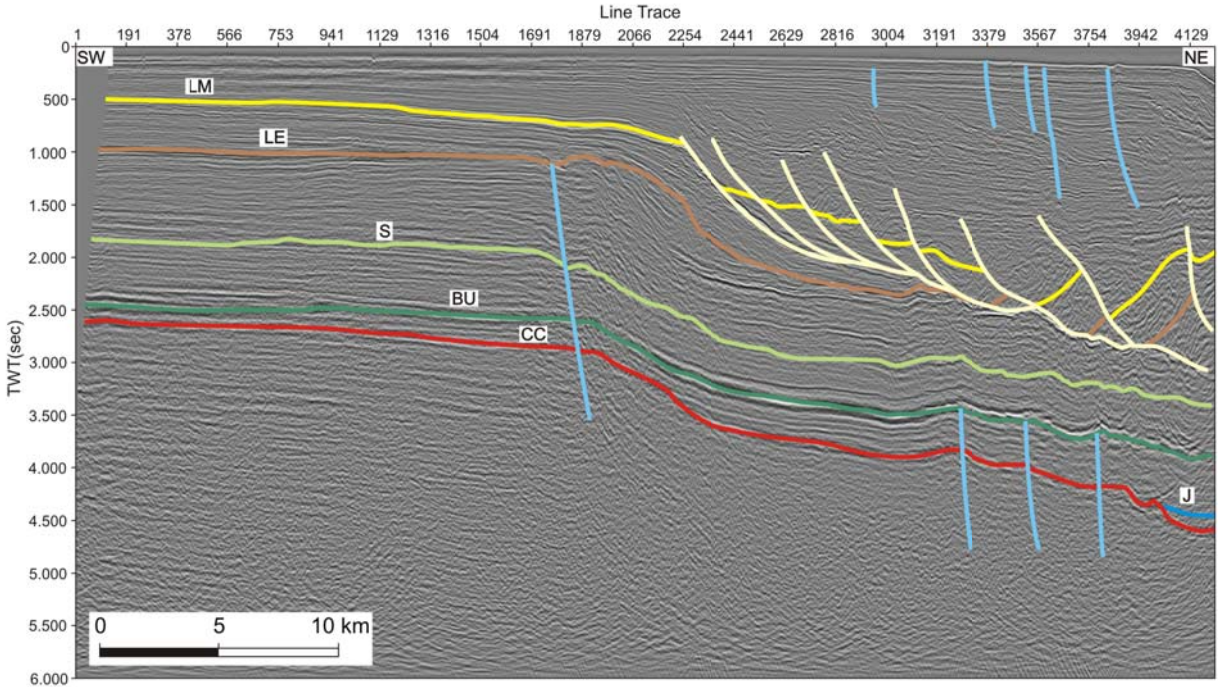
Line Trace
1
191
378
566
753
941
1129
1316
1504
1691
1879
2066
2254
2441
2629
2816
3004
3191
3379
3567
3754
3942
4129
SW
NE
LM
LE
S
BU
CC
J
TWT(sec)
0
500
1.000
1.500
2.000
2.500
3.000
3.500
4.000
4.500
5.000
5.500
6.000
0
5
10 km

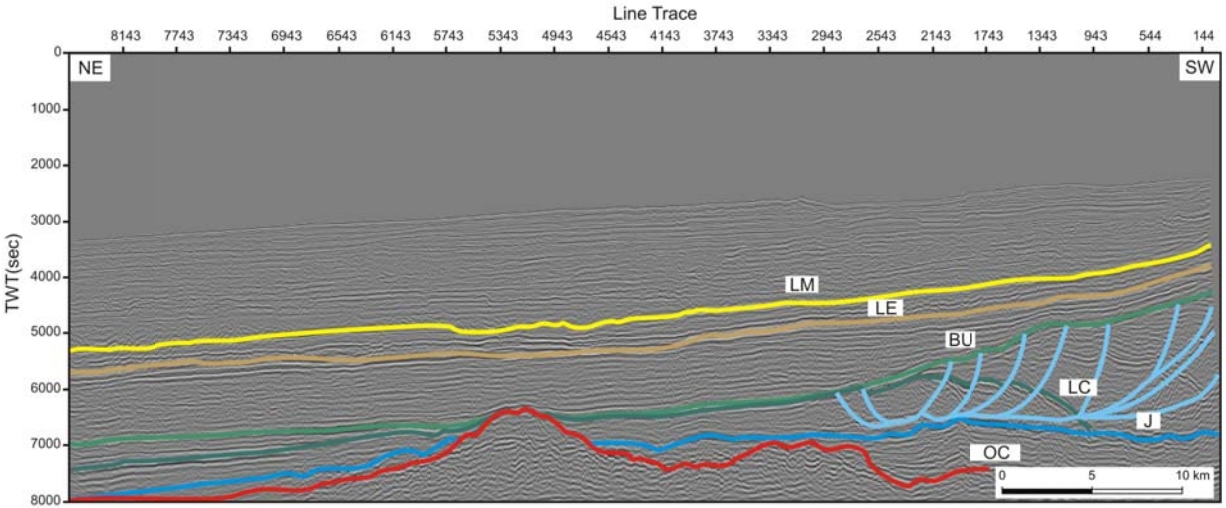
Line Trace
8143
7743
7343
6943
6543
6143
5743
5343
4943
4543
4143
3743
3343
2943
2543
2143
1743
1343
943
544
144
NE
SW
TWT(sec)
0
1000
2000
3000
4000
5000
6000
7000
8000
LM
LE
BU
LC
J
OC
0
5
10 km

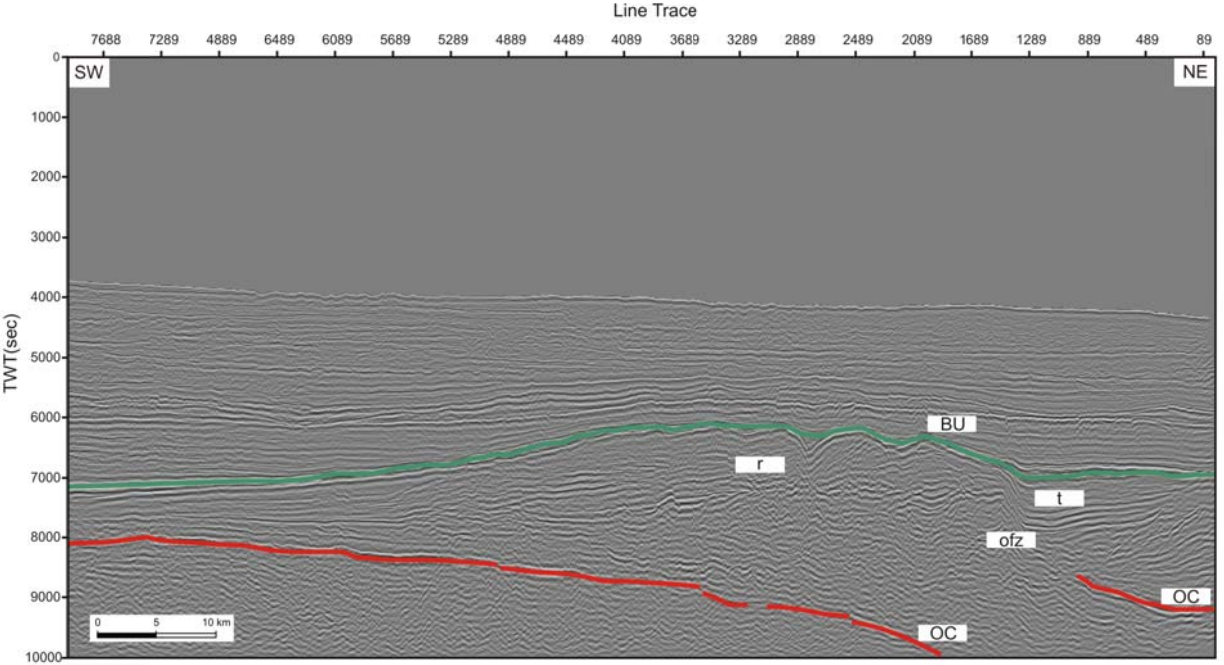
Line Trace
7688
7289
4889
6489
6089
5689
5289
4889
4489
4089
3689
3289
2889
2489
2089
1689
1289
889
489
89
SW
NE
TWT(sec)
0
1000
2000
3000
4000
5000
6000
7000
8000
9000
10000
BU
r
t
ofz
OC
OC
0
5
10 km

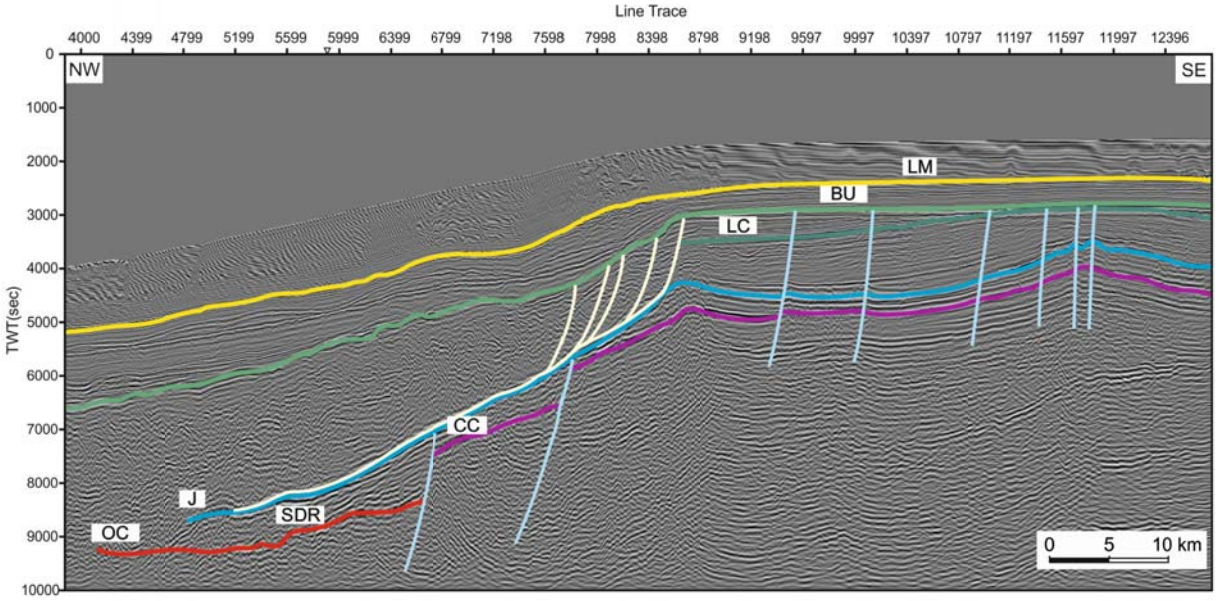
Line Trace
4000
4399
4799
5199
5599
5999
6399
6799
7198
7598
7998
8398
8798
9198
9597
9997
10397
10797
11197
11597
11997
12396
NW
SE
TWT(sec)
0
1000
2000
3000
4000
5000
6000
7000
8000
9000
10000
LM
BU
LC
CC
J
SDR
OC
0
5
10 km

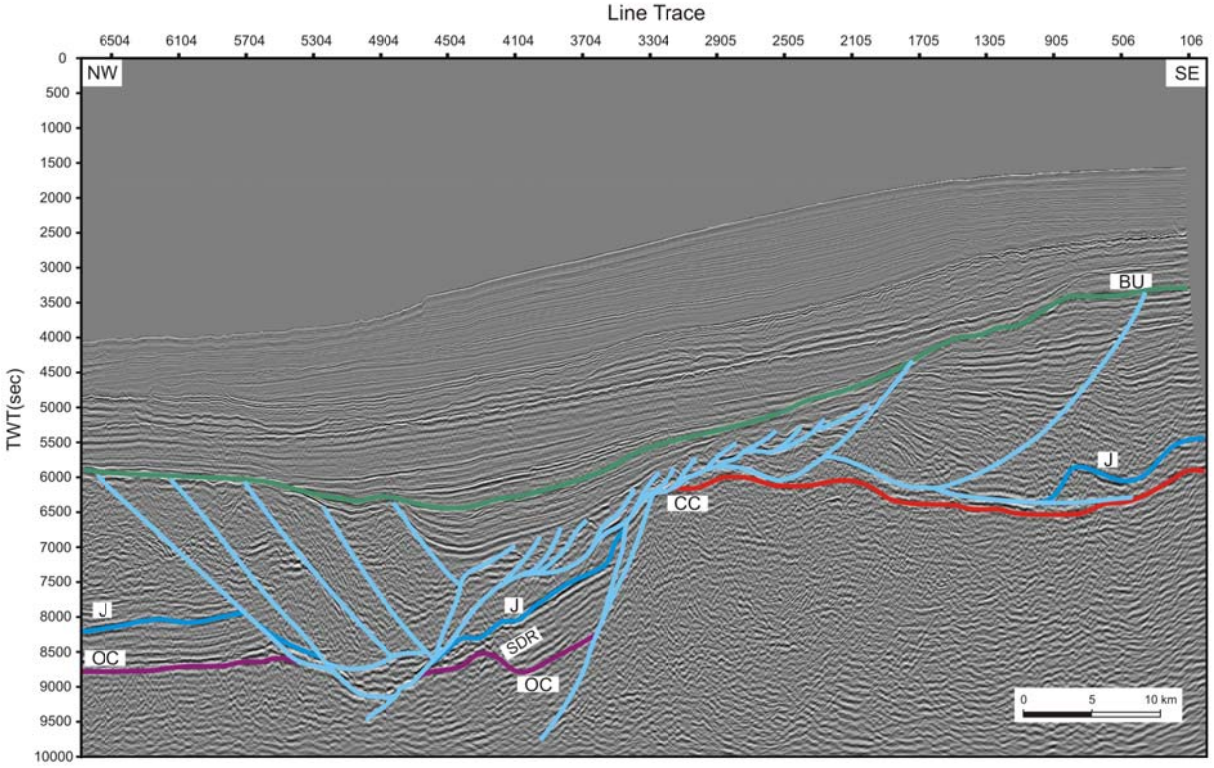
Line Trace
6504
6104
5704
5304
4904
4504
4104
3704
3304
2905
2505
2105
1705
1305
905
506
106
NW
SE
TWT(sec)
0
500
1000
1500
2000
2500
3000
3500
4000
4500
5000
5500
6000
6500
7000
7500
8000
8500
9000
9500
10000
BU
J
CC
J
J
OC
SDR
OC
0
5
10 km

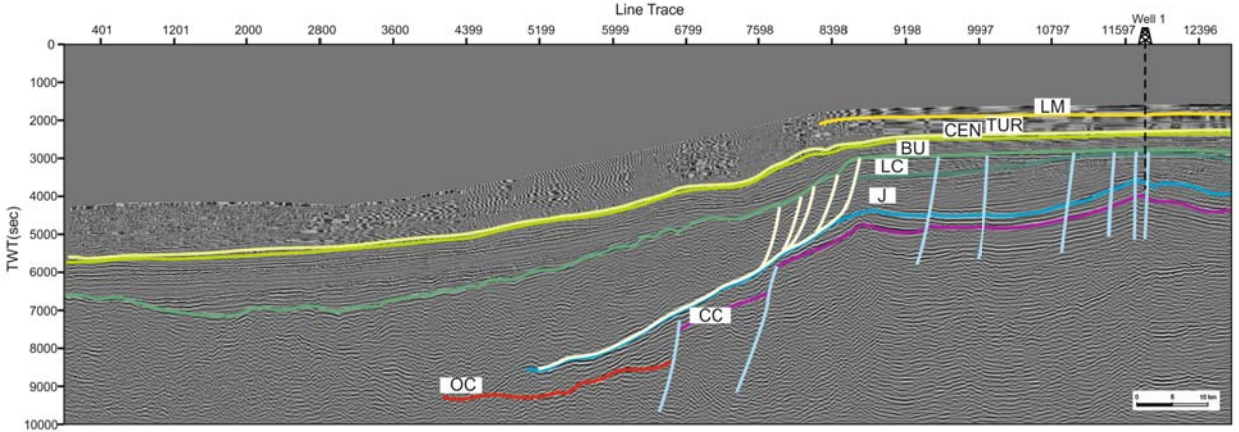
Line Trace
401
1201
2000
2800
3600
4399
5199
5999
6799
7598
8398
9198
9997
10797
11597
12396
Well 1
TWT(sec)
0
1000
2000
3000
4000
5000
6000
7000
8000
9000
10000
LM
CEN
TUR
BU
LC
J
CC
OC

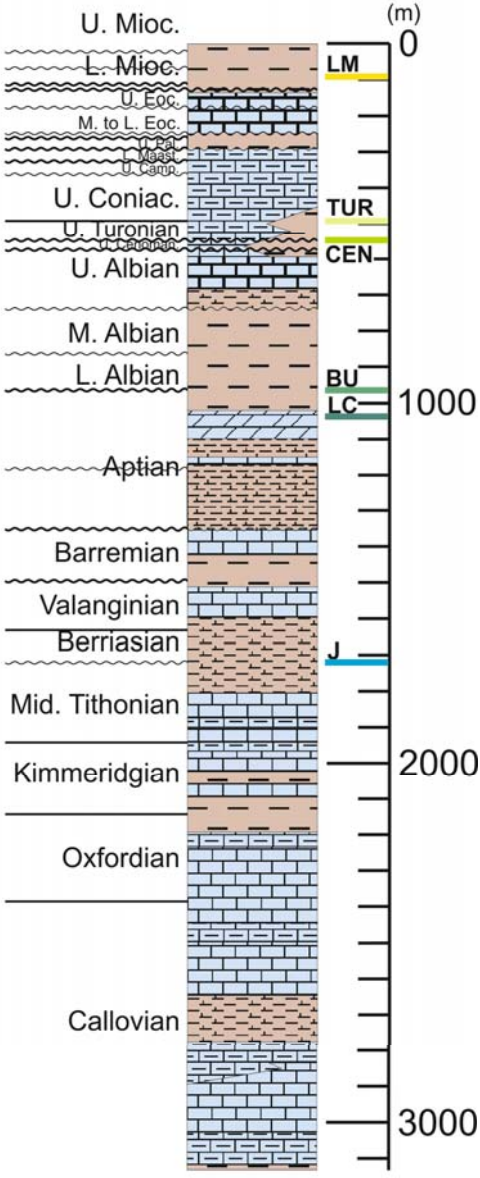
U. Mioc.
L. Mioc.
U. Eoc.
M. to L. Eoc.
U. Pal.
Maast.
U. Camp.
U. Coniac.
U. Turonian
U. Albian
M. Albian
L. Albian
Aptian
Barremian
Valanginian
Berriasian
Mid. Tithonian
Kimmeridgian
Oxfordian
Callovian
(m)
0
LM
TUR
CEN
BU
LC
1000
J
2000
3000

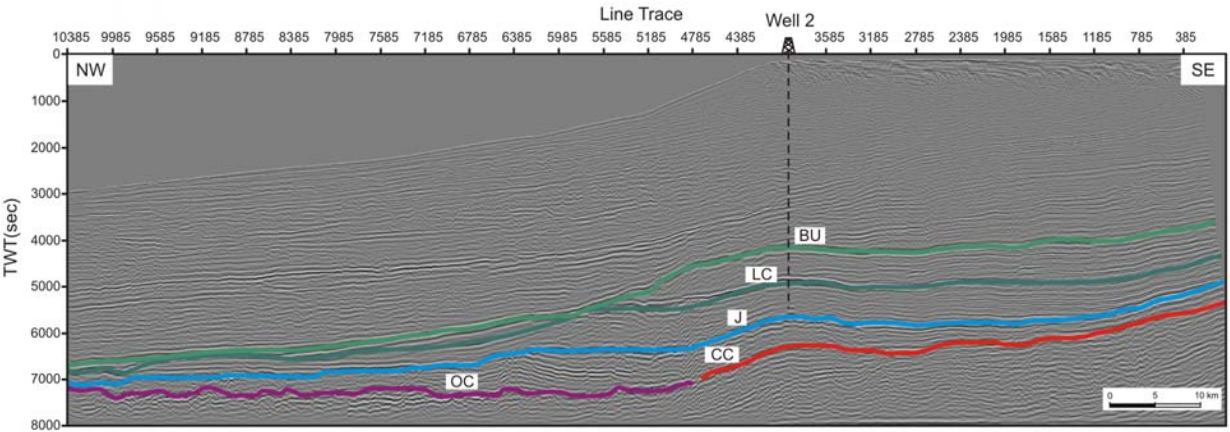
Line Trace
Well 2
10385 9985 9585 9185 8785 8385 7985 7585 7185 6785 6385 5985 5585 5185 4785 4385 3585 3185 2785 2385 1985 1585 1185 785 385
NW
SE
TWT(sec)
0
1000
2000
3000
4000
5000
6000
7000
8000
BU
LC
J
CC
OC
0 5 10 km

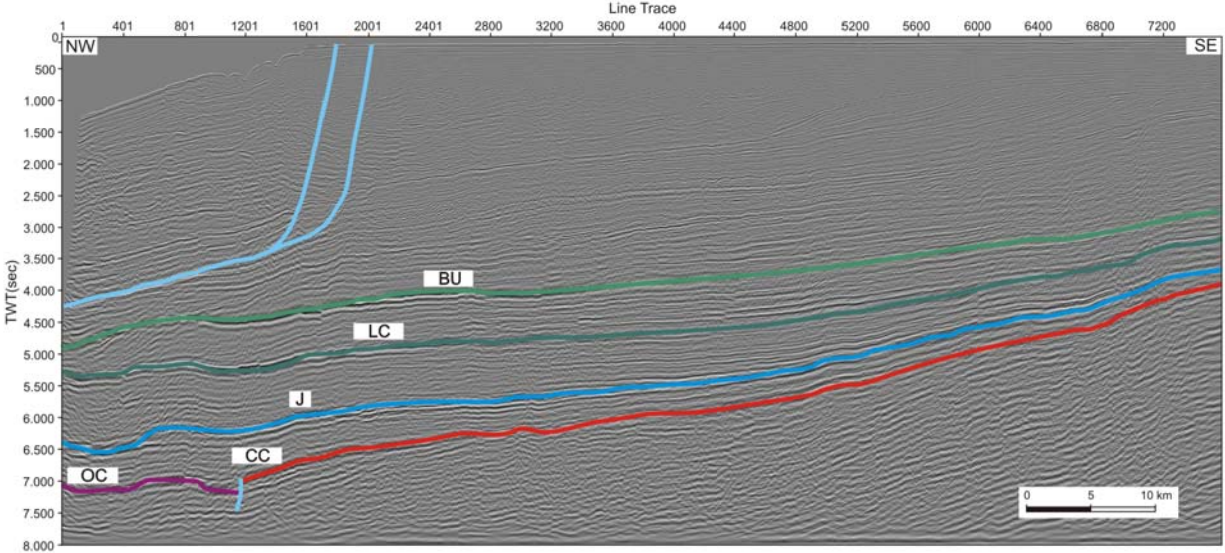
Line Trace
1
401
801
1201
1601
2001
2401
2800
3200
3600
4000
4400
4800
5200
5600
6000
6400
6800
7200
NW
SE
TWT(sec)
0
500
1.000
1.500
2.000
2.500
3.000
3.500
4.000
4.500
5.000
5.500
6.000
6.500
7.000
7.500
8.000
BU
LC
J
CC
OC
0
5
10 km

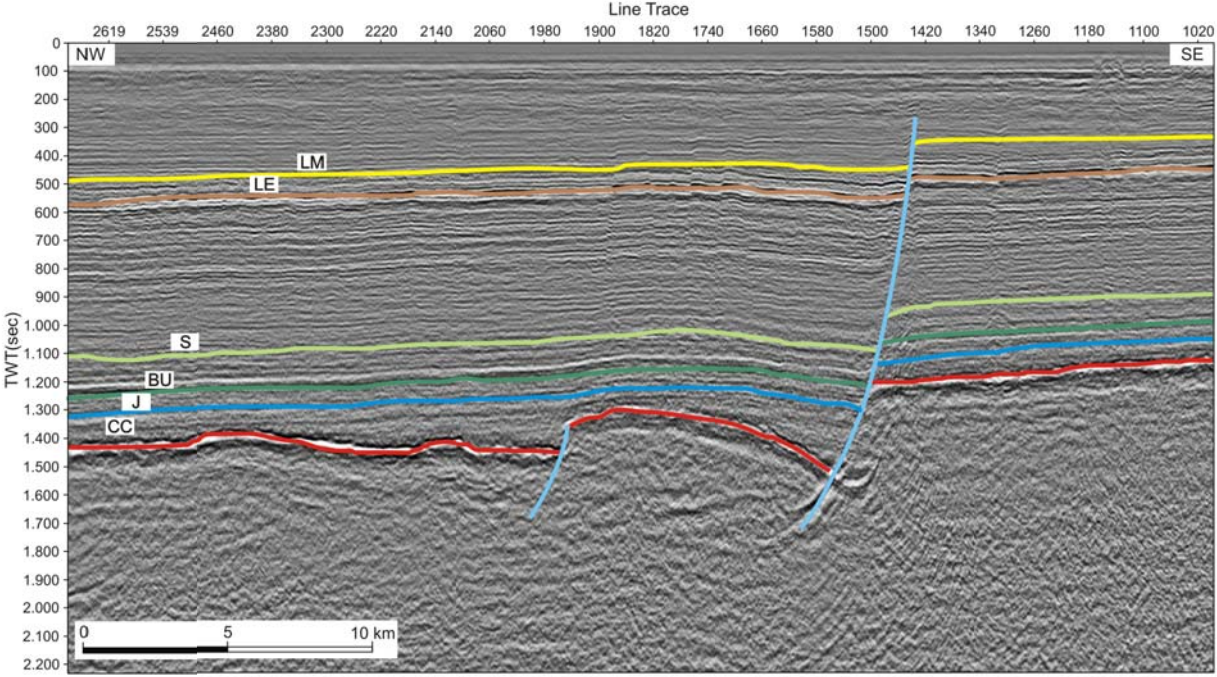
Line Trace
2619 2539 2460 2380 2300 2220 2140 2060 1980 1900 1820 1740 1660 1580 1500 1420 1340 1260 1180 1100 1020
NW
SE
TWT(sec)
0 100 200 300 400 500 600 700 800 900 1.000 1.100 1.200 1.300 1.400 1.500 1.600 1.700 1.800 1.900 2.000 2.100 2.200
LM
LE
S
BU
J
CC
0 5 10 km

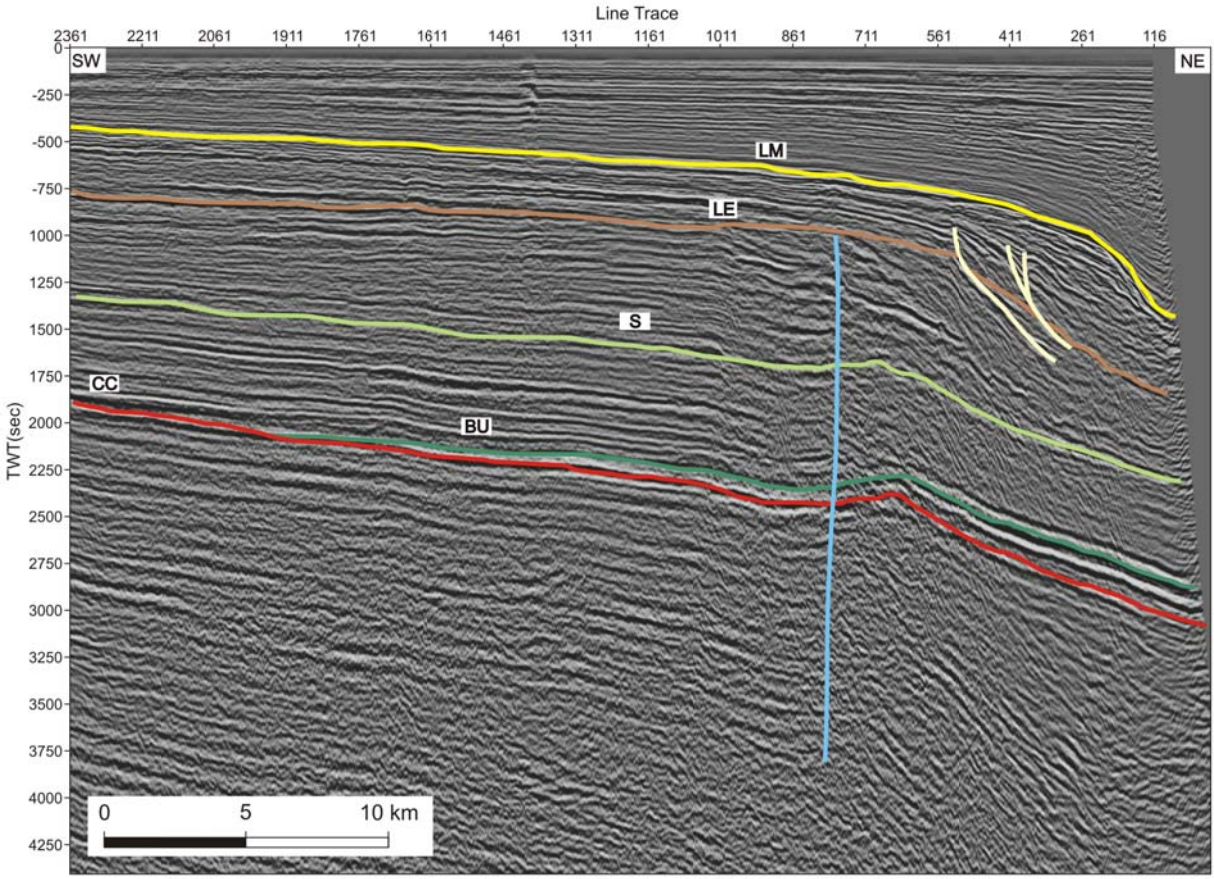
Line Trace
2361
2211
2061
1911
1761
1611
1461
1311
1161
1011
861
711
561
411
261
116
SW
NE
LM
LE
S
CC
BU
TWT(sec)
0
-250
-500
-750
1000
1250
1500
1750
2000
2250
2500
2750
3000
3250
3500
3750
4000
4250
0
5
10 km

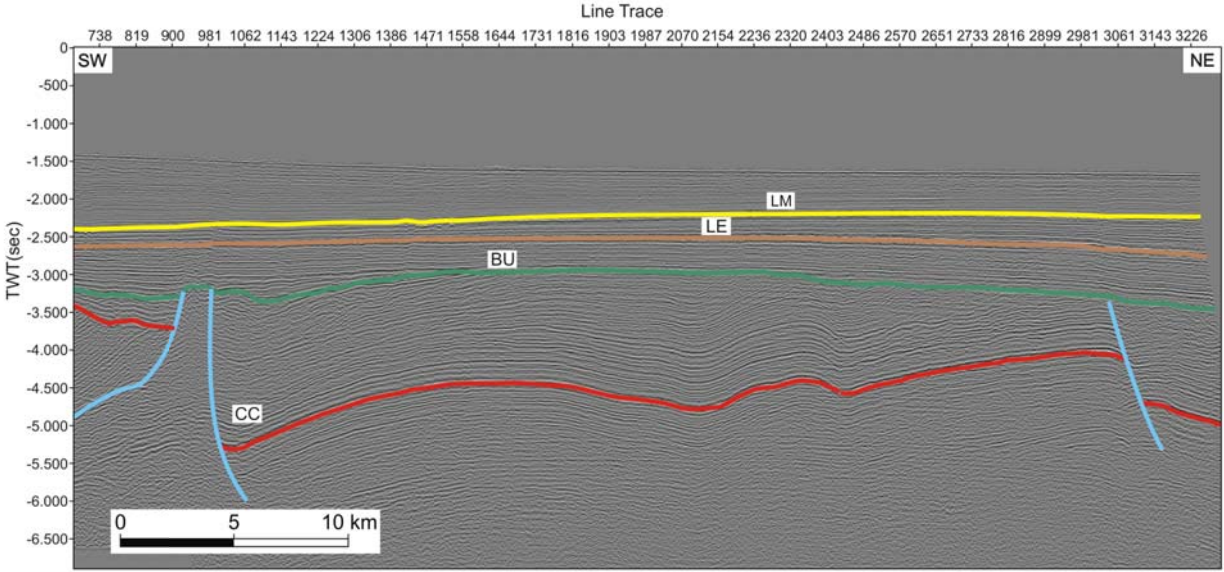
Line Trace
738 819 900 981 1062 1143 1224 1306 1386 1471 1558 1644 1731 1816 1903 1987 2070 2154 2236 2320 2403 2486 2570 2651 2733 2816 2899 2981 3061 3143 3226
SW
NE
0
-500
-1.000
-1.500
-2.000
-2.500
-3.000
-3.500
-4.000
-4.500
-5.000
-5.500
-6.000
-6.500
TWT(sec)
LM
LE
BU
CC
0
5
10 km

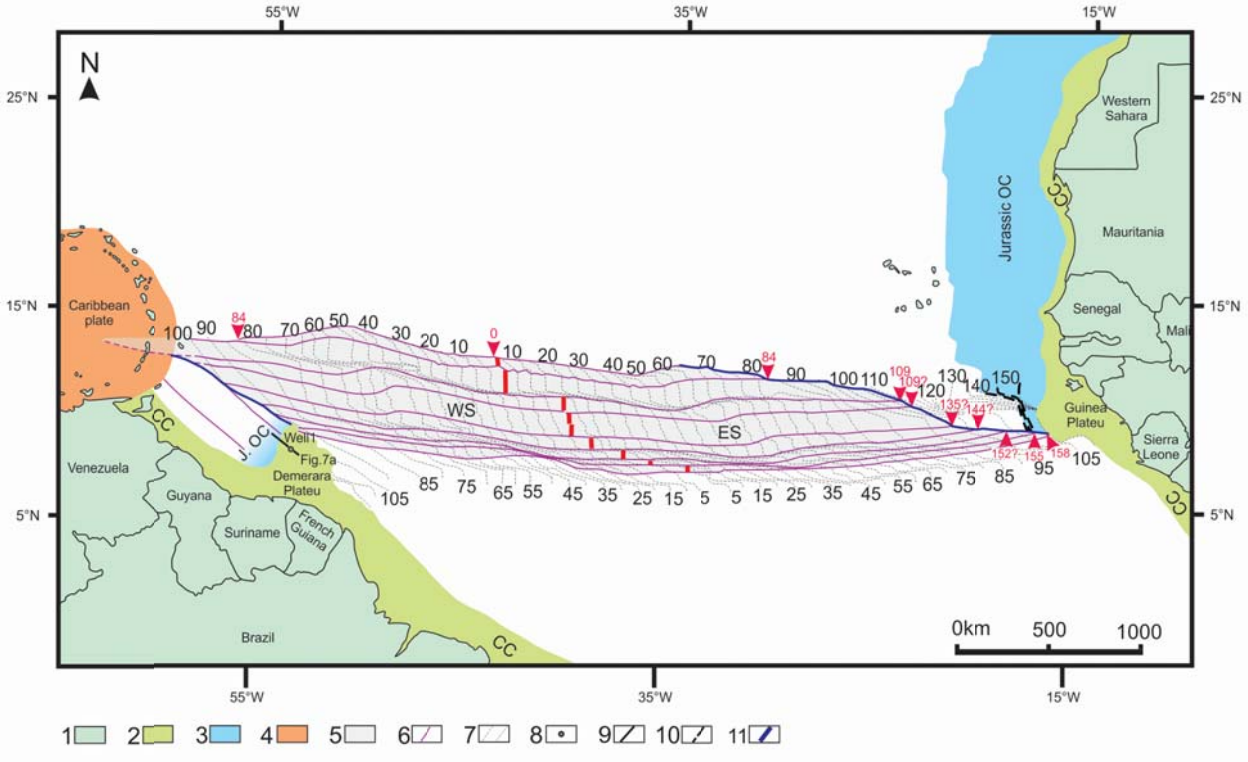
55°W
35°W
15°W
N
25°N
15°N
5°N
Caribbean plate
Venezuela
Guyana
Suriname
French Guiana
Brazil
Demerara Plateu
J. OC
Well1
Fig.7a
WS
ES
CC
Jurassic OC
Western Sahara
Mauritania
Senegal
Mali
Guinea Plateu
Sierra Leone
0km
500
1000
1
2
3
4
5
6
7
8
9
10
11

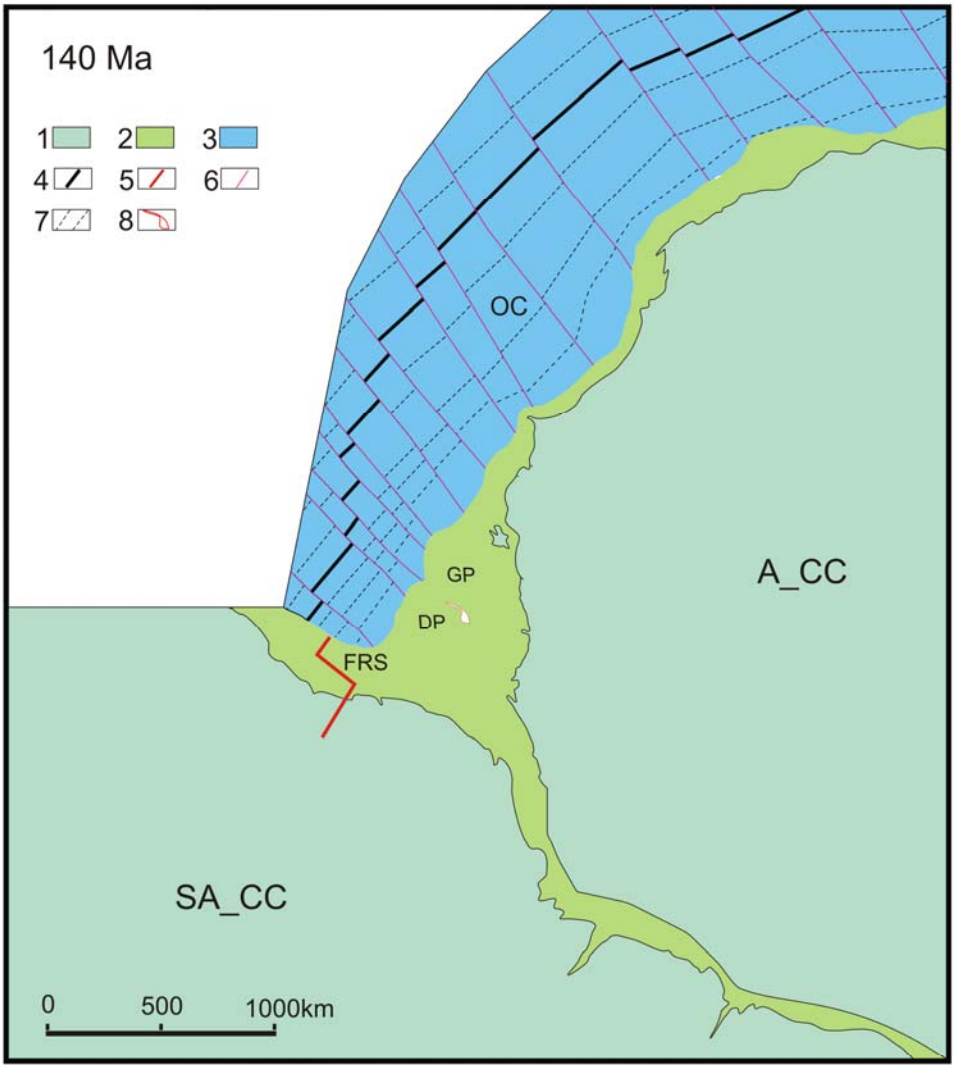
140 Ma
1
2
3
4
5
6
7
8
OC
GP
DP
FRS
A_CC
SA_CC
0
500
1000km

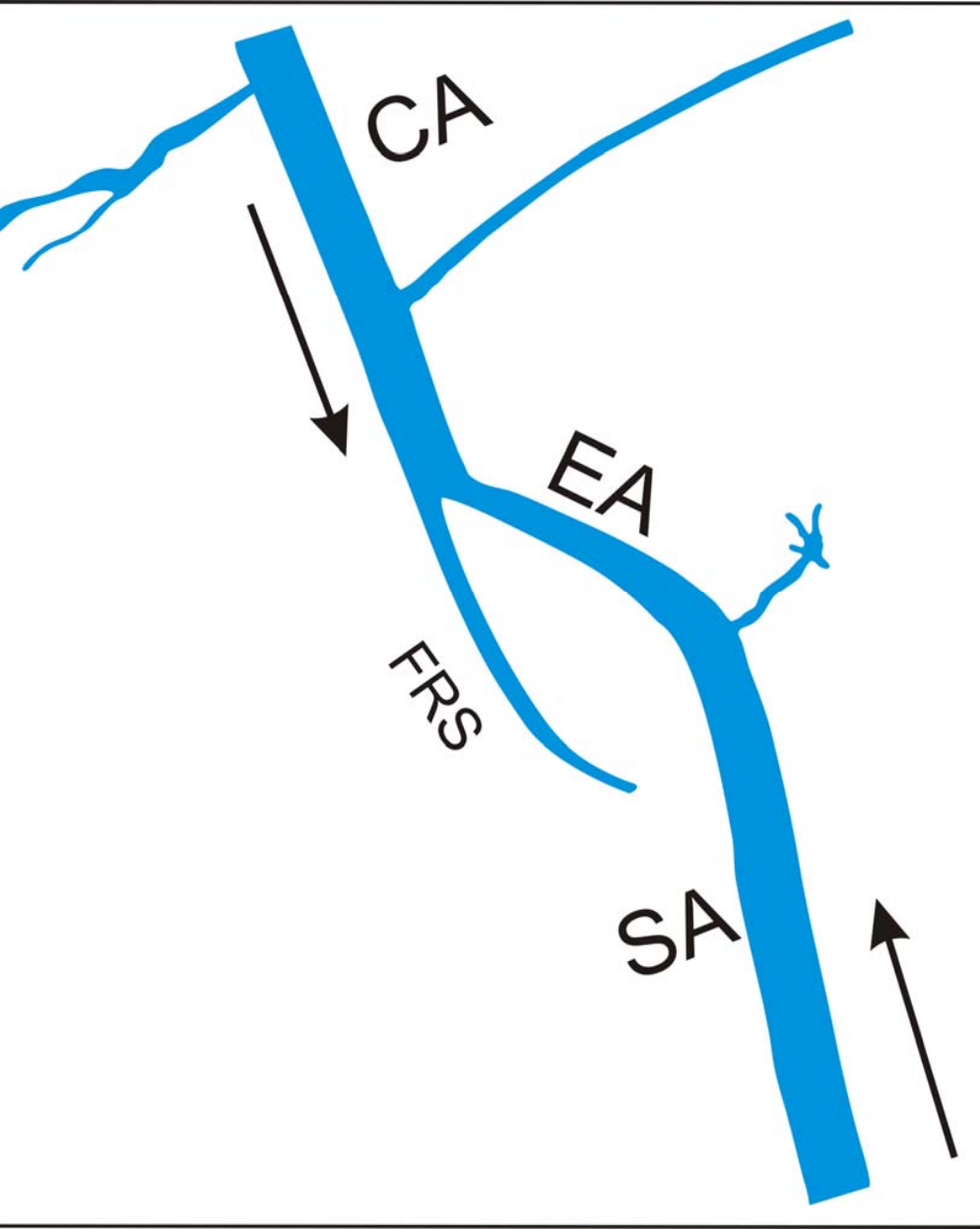
CA
EA
FRS
SA